Island size distributions in submonolayer growth with mobile islands and breakup

I. Koponen,* M. Rusanen, and J. Heinonen
Helsinki Institute of Physics, P.O. Box 9, FIN-00014 University of Helsinki, Helsinki, Finland
(Received 17 March 1998)

Island growth in the submonolayer regime with mobile islands and breakup is studied by computer simulations. It is shown that during the initial stages of growth, a scaling description similar to irreversible growth applies, but eventually the growth attains a quasistationary state where aggregation is affected by breakup and a new scaling behavior occurs. A generalized scaling description that bridges the initial and final stages of growth is presented and its validity is confirmed by simulations. [S1063-651X(98)12009-3]

PACS number(s): 07.05.−t, 68.55.−a, 68.35.Fx, 36.40.Sx

Island growth on surfaces during submonolayer deposition has received considerable attention, because it is the basic element of all further growth. By studying the scaling properties of island size distributions valuable information of microscopic surface processes can be obtained [1,2]. The primary interest has been on the role of adatom diffusion on growth [1–3], but recently also the more complicated cases of growth with mobile islands [4–6] and reversible growth with adatom detachment [7,8] have been studied. An interesting special case that has received little attention is island growth under conditions where islands are mobile and dissociation or breakup of islands occur. This problem is also of practical interest, because it is assumed to be one of the mechanisms affecting growth in ion beam assisted deposition (IBAD), where energetic ion beams are utilized in thin film growth [9].

Island growth with mobile islands and breakup is modeled here as an aggregation-breakup process $A_i+A_j \rightleftharpoons A_{i+j}$ of clusters of size i and j with the rates of aggregation and breakup specified by reaction kernels $K(i,j)$ and $F(i,j)$, respectively. Extending the well known approach used for a sourceless aggregation-breakup problem [10–13] we write the rate equations for the areal density n_s of islands of size $s \geqslant 1$ in the form

$$\frac{dn_s}{dt} = \Phi \delta_{1,s} + \frac{1}{2}\sum_{i+j=s} [K(i,j)n_i n_j - F(i,j)n_s] - \sum_{j=1}^{\infty} [K(s,j)n_s n_j - F(s,j)n_{s+j}], \quad (1)$$

where the source Φ is the deposition flux of adatoms in units of monolayers per second (ML/s). The aggregation kernel for mobile islands with a diffusion constant D_i is given by the Smoluchowski formula $K(i,j) \propto (D_i + D_j)$ [14] where the dependence on the island size can be omitted without loss of generality for point islands [6]. In cases of interest to us the diffusion coefficients of the islands follow an inverse power law $D_i \propto i^{-\mu}$ with μ in the range $1 \leqslant \mu \leqslant 2$ [15], which gives the aggregation kernel $K(i,j) \propto (i^{-\mu} + j^{-\mu})$. The breakup rate $F(i,j)$ of islands of size $s=i+j$ is taken to depend on the island size as $F(i,j) \propto (i+j)^{\alpha}$ and only binary breakup is allowed, which with $-1/2 \leqslant \alpha \leqslant 0$ is a reasonable choice for IBAD [16]. With these definitions $K(i,j) \equiv K_0 \varphi(i,j)$ and $F(i,j) \equiv F_0 \phi(i,j)$, with $\varphi(i,j) = i^{-\mu} + j^{-\mu}$ and $\phi(i,j) = (i+j)^{\alpha}$ are homogeneous kernels of order $-\mu$ and α, respectively [10,11], and with $\mathcal{R} = K_0/\Phi$ and $\kappa = F_0/K_0$ they are the input parameters specifying the model.

We have simulated island growth as described by Eqs. (1) by using the particle coalescence method (PCM) [17]. In the following we give only a brief overview of the method, because its application on aggregation [17] and aggregation with breakup (without source) [10,11,13] is explained in detail elsewhere. In the PCM, islands are defined to be point-like, and they occupy single lattice sites. When two clusters i and j jump to the same lattice site, they aggregate to a new cluster $i+j$ with a probability proportional to $K(i,j)$ [17]. The particle at a given lattice site is allowed to jump either to the nearest neighbor sites only (the NN rule) or to any site on the lattice (the MF rule), which corresponds to the mean field (MF) limit. By using the NN rule we can take into account the spatial fluctuations in n_s, as explained in more detail in Ref. [17]. Similar rules are used also for breakup by placing one of the fragments either in a nearest neighbor (NN) site or at any site chosen randomly (MF) [10,11]. The lattice size was chosen to be 500×500 and averages were carried over by 100–200 runs. Some of the calculations were performed for smaller lattices to rule out the finite size effects. The MF limit results of PCM were checked by solving in some representative cases the rate equations numerically using an adaptive Adam's method. The results for the NN rule were checked by repeating some of the calculations with the kinetic Monte Carlo (KMC) method for point islands by generalizing the hybrid simulation method introduced by Bartelt and Evans [1].

Scaling of the island size distributions n_s is discussed conveniently by introducing the distribution function $p(s,\theta) = s n_s(\theta)/\theta$, which at the coverage $\theta = \Phi t = \Sigma_{s \geqslant 1} s n_s$ gives the probability that an atom selected at random belongs to an island of size s [2,12]. After the initial stage the scale for the distribution n_s is specified by the average size $\overline{s}(\theta) = \Sigma_{s \geqslant 1} s p(s,\theta)$ and then the distribution attains the scaling form $p(s,\theta) = \overline{s}^{-1} g(s/\overline{s})$ [1,2], where the scaling function $g(x)$ with $x = s/\overline{s}$ becomes independent of the coverage θ and of the parameters $\mathcal{R} = K_0/\Phi$ and $\kappa = F_0/K_0$ [2,12]. At

*Electronic address: ismo.koponen@helsinki.fi

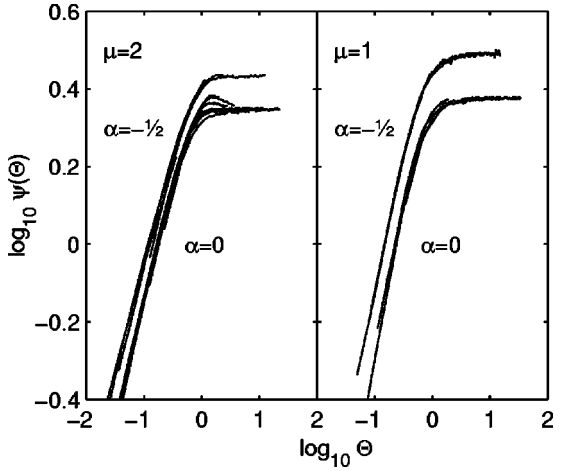

FIG. 1. Scaling function $\psi(\Theta)$ for the models with homogeneity exponents $(\mu,\alpha)=(2,0)$ and $(2,-1/2)$ (left panel) and $(\mu,\alpha)=(1,0)$ and $(1,-1/2)$ (right panel). In all cases $y=(\alpha+\mu+2)^{-1}$ gives the best data collapse. In the steady state $\psi(\Theta)\to\psi_0$, with ψ_0 given in Table I. The exponent β reported in Table I is obtained from the power law fits to the scaling function $\psi(\Theta)\propto\Theta^{\omega}$ at $\Theta<1$, where $\omega=\beta-y$.

this stage of growth the total areal density of islands $N=\Sigma_{s>1}n_s$ also follows a scaling form and obeys the relation $\overline{s}N\simeq\zeta\theta$, where the coefficient $\zeta=\int dx x^{-1}g(x)$ depends only on the function $g(x)$ [2,12].

The island size distribution is determined completely by $g(x)$ provided that the average size $\overline{s}$ is specified. It is known that in irreversible growth the average size scales as $\overline{s}\propto\mathcal{R}^{\gamma}\theta^{\beta}$, where $\beta=2/3$ in point island models [1] and the scaling exponent γ is related to the surface diffusion processes [2,4–8]. On the other hand, in sourceless aggregation with breakup the scaling of $\overline{s}$ with respect the relative breakup rate obeys the relation $\overline{s}\propto\kappa^{-y}(a/b)^{y}$, where the scaling exponent y depends only on the homogeneity exponents and it is given by $y=(\alpha+\mu+2)^{-1}$ [10,11]. The coefficients a and b as derived by Sorensen, Zhang, and Taylor (SZT) [12] are given by the integrals $a=\int dx\int dy xy\phi(x,y)g(x)g(y)$ and $b=\int dx\int dy xy\varphi(x,y)g(x+y)$. The SZT method can be applied also to the present problem, and it can be shown that a generalized scaling description that bridges these two regions of growth is (compare with the scaling description in Ref. [11])

$$\overline{s}(\Theta)=(\kappa/\theta_c)^{-y}\Theta^{y}\psi(\Theta);\quad \Theta=\theta/\theta_c, \tag{2}$$

where $\psi(\Theta)=\Theta^{\omega}$ with $\omega=\beta-y$ for $\Theta\ll 1$ and $\psi(\Theta)\to\psi_0$ with $\psi_0\propto(a/b)^{y}$ for $\Theta\gg 1$, and the crossover between these two stages of growth is determined by parameter $\theta_c\simeq\mathcal{R}^{-\gamma/\omega}\kappa^{-y/\omega}$. In the later stage where breakup affects the growth $\overline{s}(\Theta)\propto\Theta^{y}$ and it thus increases with the coverage much slower than in irreversible growth. However, within the present model breakup is not dominant enough to keep $\overline{s}$ constant.

The function $\psi(\Theta)$ for the generalized scaling is given in Fig. 1 for several PCM simulations by using the MF and NN rules, and with parameters in the range $10^{-7}\leqslant\kappa\leqslant 10^{-5}$ and $0.5\times 10^{5}\leqslant\mathcal{R}\leqslant 2\times 10^{6}$. The validity of the generalized scaling is confirmed by the observation that in all cases the scaled data collapse to a single curve. Only during the transition that occurs at $\Theta=\theta/\theta_c\approx 1$ are there deviations from the scaling function $\psi(\Theta)$. At large values $\Theta>1$ the scaling function attains a constant value ψ_0 given in Table I and it obeys the relation $\psi_0\propto(a/b)^{y}$, where a and b are calculated numerically by using $g(x)$, to be specified later on. The scaling of the total island density N was examined by plotting the function $\zeta(\theta)=\overline{s}N/\theta$. After the initial transient stage N attains a scaling form, which is signaled by ζ approaching a constant value. These values are given in Table I and they are comparable to values obtained numerically from the function $g(x)$.

TABLE I. Scaling exponents y, β, γ, and δ and the numerical constants ψ_0 and ζ (as defined in the text) obtained from the simulations. The value of y is obtained from the MF relation $y=(\alpha+\mu+2)^{-1}$. The pair (μ,α) specifies the homogeneity exponents of the aggregation and breakup kernels, respectively, and they are the input parameters of the model.

(μ,α)	y	β	γ	δ	ψ_0	ζ
(2,0)	0.250	0.87	0.52	3.0	2.22	1.32
$(2,-\frac{1}{2})$	0.286	0.88	0.53	2.7	2.71	1.34
(1,0)	0.333	1.12	0.63	2.0	2.38	1.50
$(1,-\frac{1}{2})$	0.400	1.13	0.59	1.6	3.10	1.63

In the steady state $\Theta\gg 1$ data collapse is obtained with the scaling exponent $y=(\alpha+\mu+2)^{-1}$, as predicted by the MF theory [10,11]. The exponent $\omega=\beta-y$ measured from the scaling plot yields the dynamic exponents β given in Table I. For $\mu=2$ and $\mu=1$ we obtain $\beta\approx 0.9$ and 1.1, respectively, which due to island mobility are larger than $\beta=2/3$ for the point island model with mobile adatoms only [1]. The scaling exponents γ reported in Table I are consistent with values found in models where detachment occurs easily [7], but are systematically larger than values obtained in previous

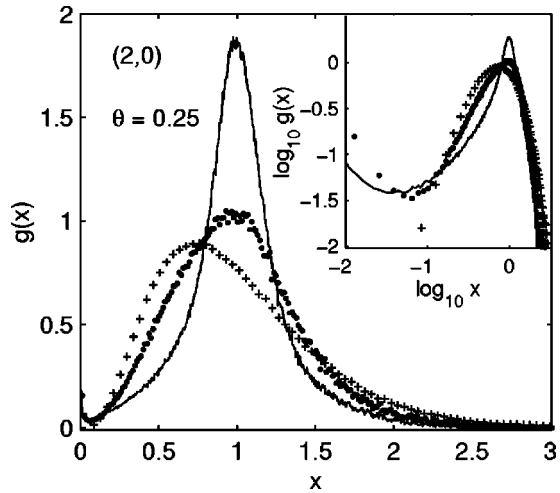

FIG. 2. Scaling function $g(x)=\overline{s}p(s,\theta)$ with $x=s/\overline{s}$ for model $(\mu,\alpha)=(2,0)$ without breakup $\kappa=0$ (solid line), with $\kappa=10^{-7}$ (●) and $\kappa=10^{-5}$ (+). In all cases $\mathcal{R}=2\times 10^{6}$ and the coverage is $\theta=0.25$. In the inset the same distributions are shown on a log-log scale.

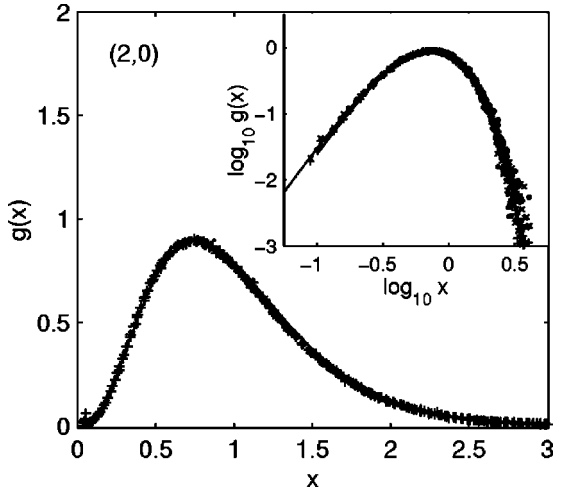

FIG. 3. Scaling functions $g(x)$ for model $(\mu,\alpha)=(2,0)$ with $\kappa=10^{-6}$ and $\mathcal{R}=2\times10^{6}$, and $\kappa=10^{-5}$ with $\mathcal{R}=0.5\times10^{6}$, 1×10^{6}, and 2×10^{6}. Distributions are given for coverages $\theta=0.1$, 0.15, 0.20, and 0.25. The fit $g(x)\propto x^{\delta}\exp(-cx)$ with the exponent δ given in Table I drawn in the figure is indistinguishable from the simulation results. The inset displays the results of KMC simulations (●), PCM simulations with NN (+), and MF (×) rules and numerical solutions to the rate equations (thin solid line) for $\kappa=10^{-5}$ and $\mathcal{R}=1\times10^{6}$. The fit is given by the thick solid line. Due to good data collapse the different results are nearly indistinguishable from the figure.

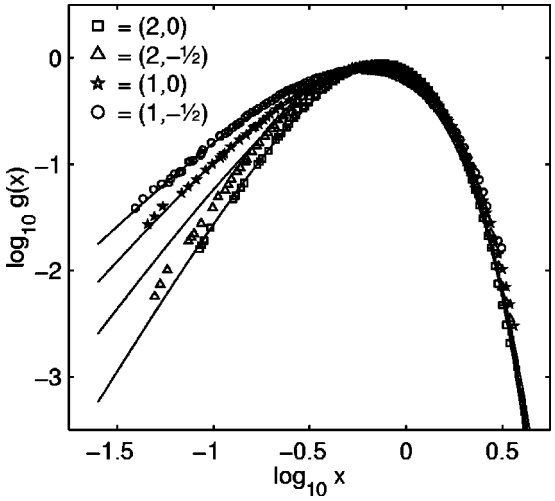

FIG. 4. Scaling functions $g(x)$ for models $(\mu,\alpha)=(2,0)$ and (1,0) and $(2,-0.5)$ and $(1,-0.5)$. Averages over simulation results for coverages $\theta=0.1$, 0.15, 0.2, and 0.25 are given by unconnected symbols. The statistical variation of the averages is of the size of the symbols. Solid lines display the fits with exponents δ given in Table I.

KMC simulations with mobile islands only where values in range $0.35<\gamma<0.42$ were obtained [4,5].

The scaling function $g(x)$ for the model $(\mu,\alpha)=(2,0)$ displayed in Fig. 2 for the relative breakup rate in the range $0\leqslant\kappa\leqslant10^{-5}$ demonstrates how $g(x)$ gradually broadens with increasing κ. In the inset of Fig. 2 the distributions are shown on a log-log scale, where the distribution of small island sizes and its disappearance with increasing κ is better seen. It is obvious that with $\kappa\to0$ the distribution $g(x)$ approaches continuously the distribution obtained for aggregation only. On the other hand, with an increasing breakup rate κ the distribution $g(x)$ becomes less sensitive to κ and its scaling is improved until it finally attains a limiting shape. This behavior is demonstrated in Fig. 3 for model $(\mu,\alpha)=(2,0)$, where it becomes obvious that $g(x)$ follows scaling with $\mathcal{R}$ and θ. The limiting scaling function in Fig. 3 has the form $g(x)\propto x^{\delta}\exp(-cx)$, which is similar to the scaling function obtained in aggregation with breakup without source [10,11]. However, the value of δ given in Table I is clearly smaller than the MF prediction $\delta=2+\mu$ obtained for the sourceless case [11], but this is to be expected because the deposition of adatoms (source) increases the number of small islands.

The effect of the spatial fluctuations in n_s was checked by performing the PCM simulations with the MF and NN models. Only for models without breakup and with the smallest breakup rate $\kappa=10^{-7}$ the spatial fluctuations affect the distributions. For $\kappa\geqslant10^{-6}$ any difference between the MF and NN models disappeared. These results of PCM simulations were confirmed by independent calculations with the KMC method and by numerical solutions of Eq. (1) for models (2,0), $(2,-1/2)$, and (1,0). All these independent methods give scaled distributions, which are very similar within the limits of statistical variation, as demonstrated for the model (2,0) in the inset of Fig. 3. Equally good agreement was obtained for the other cases, which suggests that spatial fluctuations in n_s have only a negligible role in growth with breakup. This is in agreement with previous findings for sourceless aggregation with breakup [10,11] and for aggregation with mobile clusters [17,18], but in contrast to irreversible island growth, where spatial correlations, due to the size dependence of the propensity for islands to capture diffusing adatoms affect the growth in a fundamental way [3].

Limiting scaling functions $g(x)$ were found to exist for all models studied, and they are shown in Fig. 4. It is obvious that each function $g(x)$ is specific to the given model and each case is described by a clearly different distribution. However, only the leading part $x<1$ of the distribution is affected by breakup and island diffusion. The exponent δ (given in Table I) specifying the slope of the leading edge depends on both homogeneity exponents α and μ and with decreasing mobility (increasing μ) the slope becomes steeper (value of δ increases) as expected on the basis of the MF theory where δ also increases with μ [11]. A decrease in breakup has a similar effect of increasing the values of δ. Inspection of results given in Table I suggest that within the present model and range of homogeneity exponents, the scaling exponents β and γ are sensitive mainly to island mobility, whereas y and δ depend also on the breakup.

In summary, we have demonstrated that for island growth with island breakup the rate equations give an accurate description of the growth and predict correctly the island size distributions. A generalized scaling description was presented, which describes the initial, irreversible stage of growth and the final stage, where aggregation is affected by breakup. Scaling exponents and scaled size distributions were found to be sensitive to island mobility and breakup, which makes it possible to obtain rather detailed and unambiguous information on these surface processes by examining the scaling properties of island size distributions.

[1] M.C. Bartelt and J.W. Evans, Phys. Rev. B **46**, 12 675 (1992).
[2] G.S. Bales and D.C. Chrzan, Phys. Rev. B **50**, 6057 (1994); Phys. Rev. Lett. **74**, 4879 (1995).
[3] M.C. Bartelt and J.W. Evans, Phys. Rev. B **54**, R17 359 (1996); P.A. Mulheran and J.A. Blackman, *ibid.* **53**, 10261 (1996).
[4] P. Jensen, A.-L. Barabási, H. Larralde, S. Havlin, and H.E. Stanley, Phys. Rev. B **50**, 15 316 (1994).
[5] L. Kuipers and R.E. Palmer, Phys. Rev. B **53**, R7646 (1996).
[6] P.L. Krapivsky, J.F.F. Mendes, and S. Redner, cond-mat/9712072 (1997).
[7] C. Ratsch, A. Zangwill, P. Šmilauer, and D.D. Vvedensky, Phys. Rev. Lett. **72**, 3194 (1994).
[8] J.A. Blackman and A. Marshall, J. Phys. A **27**, 725 (1994); G.S. Bales and A. Zangwill, Phys. Rev. B **55**, R1973 (1997).
[9] C.-H. Choi, R. Ai, and S.A. Barnett, Phys. Rev. Lett. **67**, 2826 (1991); E. Chason and B.K. Kellermann, Nucl. Instrum. Methods Phys. Res. B **127–128**, 225 (1997); W. Ensinger, *ibid.* **127–128**, 796 (1997); S. Esch, M. Breeman, M. Morgenstern, T. Michely, and G. Comsa, Surf. Sci. **365**, 187 (1996).
[10] F. Family, P. Meakin, and J.M. Deutch, Phys. Rev. Lett. **57**, 727 (1986).
[11] P. Meakin and M.H. Ernst, Phys. Rev. Lett. **60**, 2503 (1988).
[12] C.M. Sorensen, H.X. Zhang, and T.W. Taylor, Phys. Rev. Lett. **59**, 363 (1987); R.D. Vigil and R.M. Ziff, Phys. Rev. Lett. **61**, 1431 (1988).
[13] T. Sintes, R. Toral, and A. Chakrabarti, Phys. Rev. A **46**, 2039 (1992); Phys. Rev. E **50**, 2967 (1994).
[14] M. von Smoluchowski, Z. Phys. Chem. (Leipzig) **92**, 129 (1917); Phys. Z. **17**, 585 (1916); M.H. Ernst, in *Fractals in Physics*, edited by L. Pietronero and E. Tosatti (Amsterdam, Elsevier, 1986), p. 289.
[15] A.F. Voter, Phys. Rev. B **34**, 6819 (1986); S.V. Khare, N.C. Bartelt, and T.L. Einstein, Phys. Rev. Lett. **75**, 2148 (1995); W.W. Pai, A.K. Swan, Z. Zhang, and J.F. Wendelken, *ibid.* **79**, 3210 (1997); L. Bitar, P.A. Serena, P. García-Mochales, N. García, and V. T. Binh, Surf. Sci. **339**, 221 (1995).
[16] J. Sillanpää and I. Koponen, Nucl. Instrum Methods Phys. Res. B **142**, 67 (1998).
[17] K. Kang and S. Redner, Phys. Rev. A **30**, 2833 (1984); Phys. Rev. Lett. **52**, 955 (1984); K. Kang, S. Redner, P. Meakin, and F. Leyvraz, Phys. Rev. A **33**, 1171 (1986).
[18] P.G.J. van Dongen and M.H. Ernst, Phys. Rev. Lett. **54**, 1396 (1985); J. Stat. Phys. **50**, 295 (1988); P.G.J. van Dongen, Phys. Rev. Lett. **63**, 1281 (1989).